Chemical Science

Dynamic Article Links

Cite this: *Chem. Sci.*, 2012, **3**, 1003

www.rsc.org/chemicalscience

EDGE ARTICLE

Synthesis of a diniobium tetraphosphorus complex by a 2(3−1) process†

Alexandra Velian and Christopher C. Cummins*

Received 16th November 2011, Accepted 18th January 2012
DOI: 10.1039/c2sc00931e

Dimer $[P_2Nb(ODipp)_3]_2$ (Dipp = 2,6-^{i}Pr$_2$C$_6$H$_3$) has been obtained *via* a novel "2(3−1)" synthetic strategy. The mononuclear diphosphorus complex $P_2Nb(ODipp)_3$ targeted for generation by formal P^- abstraction from previously reported $[Na(THF)_3][P_3Nb(ODipp)_3]$ ostensibly undergoes irreversible dimerization to form the $[P_2Nb(ODipp)_3]_2$ complex, and is alternatively trapped reversibly by 1,3-cyclohexadiene with *in situ* formation of $C_6H_8P_2Nb(ODipp)_3$. The molecular structure of $[P_2Nb(ODipp)_3]_2$ has been determined by X-ray crystallography. Computational studies provide further insights into the bonding and reactivity of $P_2Nb(ODipp)_3$, $[P_2Nb(ODipp)_3]_2$, and $C_6H_8P_2Nb(ODipp)_3$.

Introduction

While the chemistry of mononuclear acetylene complexes has blossomed since Reppe's pioneering work in the early 1940s,[1] the class of mononucler diphosphorus complexes—P_2 being the isoelectronic, isolobal and diagonal relative[2] of acetylene—has been little explored. To date, mononuclear transition-metal P_2 complexes have not been isolated,[3] but in one instance, a side-on, monometallic P_2-complex $(P_2)W(CO)_5$ has been proposed as the elimination product from $[(CO)_5W](\eta^2\text{-PPNMes*})Nb(N[Np]Ar)_3$ (Ar = 3,5-Me$_2$C$_6$H$_3$, Np = CH$_2$C(CH$_3$)$_3$, Mes* = 2,4,6-(CMe$_3$)$_3$C$_6$H$_2$).[4] The cophotolysis of P_4 with metal carbonyl complexes[5,6] leading to the formation of $(\mu_2,\eta^2\text{-}P_2)_2M_2Cp^*_2$ (M = Co, Fe)[7] and $(\mu_2,\eta^2\text{-}P_2)_2Co_2Cp''_2$ (Cp″ = C$_5$H$_3$^{t}Bu$_2$-1,3),[8] may also involve the intermediacy of mononuclear diphosphorus complexes $(P_2)MCp^R$.

Encouraged by the existence of several mononuclear alkyne complexes of group 5 transition metals, such as (PhC≡CPh)Ta(ODipp)$_3$[10] or (PhC≡CPh)Nb(N[CH$_2$^{t}Bu]Ar)$_3$,[11] we sought to access the solution chemistry of a mononuclear diphosphorus niobium complex. Specifically, a side-on P_2 adduct of Nb(ODipp)$_3$ (**1**, Dipp = 2,6-^{i}Pr$_2$C$_6$H$_3$) was targeted by proposed abstraction of P^- from the previously reported $[\mathbf{1}\text{-}P_3]^-$ anion.[9] Herein we show that the process targeting intermediate **1**-P_2 results in either irreversible formation of the isolable dimer $P_4\mathbf{1}_2$, or when 1,3-cyclohexadiene is present, reversible [2+4] Diels–Alder cycloaddition to the diene with *in situ* formation of **1**-$P_2C_6H_8$ (see Scheme 1). This pattern of reactivity parallels that observed for some organic diphosphenes, such as $[PN(SiMe_3)_2]_2$.[12]

Department of Chemistry, Massachusetts Institute of Technology, Cambridge, MA, 02139-4307. E-mail: ccummins@mit.edu

† Electronic supplementary information (ESI) available: CCDC reference number 854065. For ESI and crystallographic data in CIF or other electronic format see DOI: 10.1039/c2sc00931e

Results and discussion

IMo(N[^{t}Bu]Ar)$_3$, a potential precursor to the known PMo(N[^{t}Bu]Ar)$_3$[13] molecule and a viable salt elimination partner, was chosen as a suitable P^- abstractor for reaction with $[Na(THF)_3][\mathbf{1}\text{-}P_3]$. The reaction proceeds quantitatively in diethylether

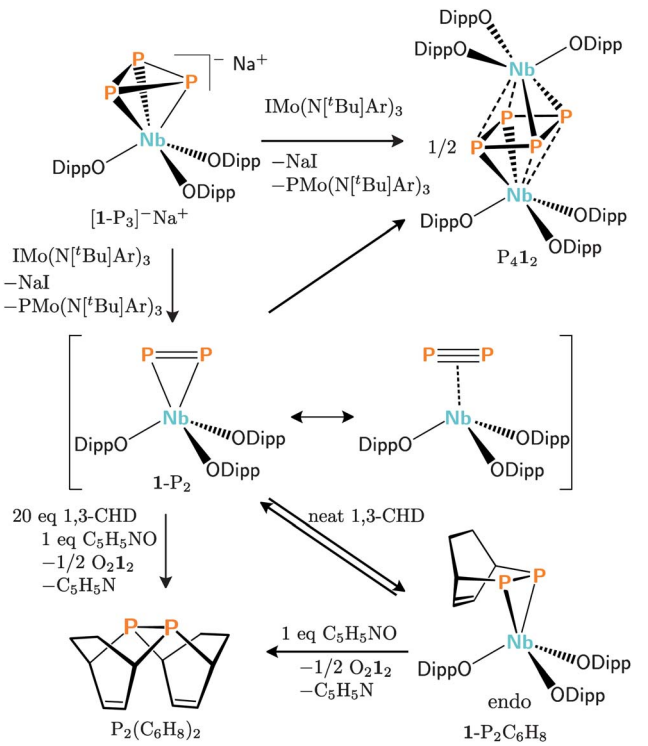

Scheme 1 Transformations of the proposed unsaturated reactive intermediate $P_2Nb(ODipp)_3$ (Dipp = 2,6-^{i}Pr$_2$C$_6$H$_3$), generated by formal abstraction of P^- from the previously reported[9] *cyclo*-P_3 anion $[P_3Nb(ODipp)_3]^-$ (1,3-CHD = 1,3-cyclohexadiene).

(5 h, 22 °C), to form the dimer $P_4\mathbf{1}_2$, PMo(N[^{t}Bu]Ar)$_3$, and NaI. We designate the formation of dimer $P_4\mathbf{1}_2$ following P$^-$ abstraction as a "2(3−1)" process thus indicating the degree *n* of catenation of the P_n ligand. PMo(N[^{t}Bu]Ar)$_3$ was separated by crystallization from THF at −35 °C and isolated in 79% yield as yellow crystals. From the mother liquor of the latter crystallization, $P_4\mathbf{1}_2$ was isolated in 71% yield as dark red crystals after replacement of THF with an *n*-pentane/Et_2O mixture and crystallization at −35 °C.

The solid-state molecular structure of $P_4\mathbf{1}_2$ incorporates a square, *cyclo*-P_4 ligand, sandwiched between the two niobium ions. This is analogous to the recently reported ($\mu_2,\eta^{4:4}$-P_4)[Zr(L_2X_2)]$_2$ complex (L_2X_2 = PhP($CH_2SiMe_2NSiMe_2CH_2$)$_2$PPh).[14] The planar *cyclo*-P_4 ligand has also been shown to bridge between two U centers, this time in a formally doubly reduced state, in ($\mu_2,\eta^{4:4}$-P_4)[U(N[^{t}Bu]Ar)$_3$]$_2$[15] and in ($\mu,\eta^{2:2}$-P_4)[U(η^5-C_5Me_5)(η^8-C_8H_6(Si^{i}Pr$_3$)$_2$-1,4)]$_2$.[16]

The *cyclo*-P_4 unit in $P_4\mathbf{1}_2$ is disordered around the Nb–Nb axis over three positions, with occupancies of 75%, 20% and 5% (see Fig. 1). The following discussion makes reference to the component having 75% occupancy. The four P atoms in $P_4\mathbf{1}_2$ are arranged in a square unit, with almost identical P–P single bonds[18] ranging from 2.230(2) to 2.250(2) Å in length. The *cyclo*-P_4 unit has a torsion angle of 0.15(9)° (P1–P2–P3–P4), and bond angles ranging from 89.31(7) to 90.80(7)°. The cesium salt of the formally dianionic P_4, as found in $Cs_2P_4\cdot 2NH_3$,[19] also displays

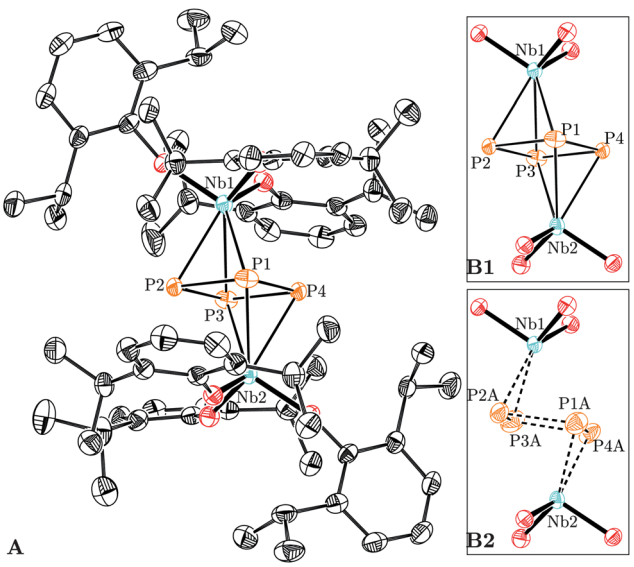

Fig. 1 Solid-state molecular structure of $P_4\mathbf{1}_2$ with ellipsoids at the 50% probability level and rendered using PLATON.[17] The *cyclo*-P_4^{4-} unit is disordered around the Nb1–Nb2 axis over three positions, with the occupancies of 75% (in B1, zoomed in), 20% (in B2, zoomed in) and 5%. In A, for clarity, only the position with 75% occupancy is displayed. Hydrogen atoms are omitted for clarity. Selected interatomic distances (Å) and angles (°): Nb1–P1 2.680(1), Nb1–P2 2.506(1), Nb1–P3 2.728(2), Nb1–P4 2.912(1), Nb2–P1 2.724(2), Nb2–P2 2.917(1), Nb2–P3 2.699(2), Nb2–P4 2.506(1), P1–P4 2.234(2), P1–P2 2.259(2), P2–P3 2.230(2), P3–P4 2.250(2), P4–P1–P2 90.46(6), P3–P2–P1 89.31(7), P2–P3–P4 90.80(7), P1–P4–P3 89.44(6), P1–P2–P3–P4 0.15(9), Nb1–P1A 2.9310(1), Nb1–P2A 2.420(5), Nb1–P3A 2.464(6), Nb1–P4A 2.9816(1), P1A–P2A 2.21(1), P1A–P4A 2.24(1), P2A–P3A 2.23(1), P3A–P4A 2.22(1), P1A–P2A–P3A–P4A 1.2(5).

a square P_4 unit, but with significantly shorter P–P interatomic distances of 2.146(1) Å. In contrast to the planarity of the *cyclo*-P_4 ligand of $P_4\mathbf{1}_2$, tetracyclophosphane rings formed by dimerization of organic diphosphenes are puckered.[20] The *cyclo*-P_4 unit in $P_4\mathbf{1}_2$ is tilted with respect to the Nb1–Nb2 axis, and interacts $\mu_2,\eta^{3:3}$ with the two niobium centers. Two short Nb–P single bonds[18] of 2.506(1) Å, and four elongated single bonds with values ranging from 2.680(1) to 2.728(2) Å are identified. The remaining two Nb–P interactions of 2.917(1) and 2.912(1) Å we regard as non-bonding.[21,22] This apparent non-equivalence of the P atoms is lost in solution, as $P_4\mathbf{1}_2$ displays a characteristic sharp singlet resonance in its $^{31}P\{^1H\}$ NMR spectrum at +124 ppm, and this signal does not broaden significantly even at −80 °C. This square, $\mu_2,\eta^{3:3}$ *cyclo*-P_4 ligand, ostensibly assembled by effective [2+2] cycloaddition of two P_2 units, is virtually identical in bond metrical parameters and the square arrangement of the phosphorus atoms with the recently reported $\mu_2,\eta^{4:4}$ *cyclo*-P_4 ligand obtained by direct activation of P_4 at a zirconium center, cited above.[14]

To better understand the Nb–P interactions, the geometry of $P_4\mathbf{1}_2$ was optimized using DFT methods.[23] The optimized structure features a rectangular *cyclo*-P_4 ligand coordinated $\mu_2,\eta^{2:2}$ between the two niobium atoms, similar to the structure observed in the second crystalline component with 20% occupancy for the disordered *cyclo*-P_4 unit (see Fig. 1, B2). The two pairs of P–P bonds interacting with the Nb centers maintain the initial length of 2.253 Å, whereas the other two P–P bonds are elongated to 2.325 Å. This $\mu_2,\eta^{2:2}$ complex is calculated to be only 1.5 kcal mol^{-1} lower in enthalpy than the $\mu_2,\eta^{3:3}$ complex, likely promoting a fluxional coordination of the *cyclo*-P_4 unit to the niobium centers. When the isopropyl groups on the ODipp ligands are replaced with hydrogen atoms, the calculated (P_4)[Nb(OPh)$_3$]$_2$ complex adopts a $\mu_2,\eta^{4:4}$ coordination of the *cyclo*-P_4 ligand between the two niobium atoms, with one Nb–P distance longer than the other three (2.786 Å *vs.* 2.531, 2.677 and 2.693 Å), suggesting that steric bulk limits the interaction of the *cyclo*-P_4 ligand with the niobium atoms.

The diamagnetism of $P_4\mathbf{1}_2$, and the single bond character of the P–P interactions in the *cyclo*-P_4 ligand supported by interatomic distances and Mayer bond orders[24] suggest that the *cyclo*-P_4 ligand is best formulated as tetraanionic. At the same time, the calculated Mulliken gross atomic charges for P are close to zero, suggesting a rather covalent interaction of the phosphorus atoms with the niobium centers.

A model for the naked **1**-P_2 putative intermediate was built from the X-ray structure of the [**1**-P_3]$^-$ anion, and optimized using DFT methods.[23,25] The calculated distance between the phosphorus atoms of 2.058 Å is typical for a P=P double bond,[27] and the corresponding Mayer bond order is calculated to be 1.58. The π symmetry and steric accessibility of the HOMO and LUMO orbitals, localized mostly on the phosphorus atoms, and the small 1.3 eV energy gap between them is consistent with what we interpret as high reactivity of **1**-P_2 (see Fig. 2).

One- or two-electron reduction of $P_4\mathbf{1}_2$ with sodium amalgam led to the fragmentation of the [P_4Nb_2] core with reformation of the [**1**-P_3]$^-$ anion, which could be recovered in 80% yield (based on P), as the [Na(THF)$_3$][**1**-P_3] salt.

In order to intercept the proposed intermediate P_2 complex prior to its dimerization, the reaction of [Na(THF)$_3$][**1**-P_3] with

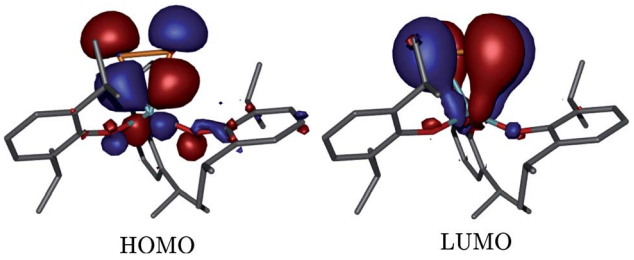

Fig. 2 The HOMO (left) and LUMO (right) orbitals of **1**-P_2, built and optimized using DFT methods[23,25] and visualized using Gabedit.[26] Selected interatomic distances (Å): P–P 2.058, Nb–P 2.485, 2.500.

$IMo(N[^tBu]Ar)_3$ was carried out in the presence of 1,3-cyclohexadiene (1,3-CHD). 1,3-Dienes have been employed frequently as cycloaddition partners with sources of P=P unsaturation.[2,6,28–31] When the reaction between $IMo(N[^tBu]Ar)_3$ and $[Na(THF)_3][$**1**-$P_3]$ was carried out in the presence of a large excess of 1,3-CHD, a new substance proposed to be the adduct of formula **1**-$P_2C_6H_8$ was formed, depending on the reaction time, in 45 to 77% spectroscopic yield as measured by inverse-gated $^{31}P\{^1H\}$ NMR spectroscopy and referenced to PPh_3 as an internal standard. This new substance displays a singlet resonance in its $^{31}P\{^1H\}$ NMR spectrum at −69 ppm. Many η^2-diphosphene complexes (η^2-$R_1P{=}PR_2$)ML_n display phosphorus shifts in this region of the ^{31}P NMR window.[31] Once formed, **1**-$P_2C_6H_8$ is stable in solution at −35 °C for at least a week, but when solutions are stored at temperatures above 0 °C, conversion to P_4**1**$_2$ is observed, along with production of a mixture of unidentified products. A 0.06 M solution of **1**-$P_2C_6H_8$ in neat 1,3-CHD has a $t_{1/2}$ = 10 h at 10 °C. Dimer P_4**1**$_2$ formed only to a small extent (*ca.* 1%) under these conditions. When a similar experiment was performed at 0 °C, P_4**1**$_2$ formed in 20% yield after 3 days. The conversion of **1**-$P_2C_6H_8$ to P_4**1**$_2$ is suggestive of the following equilibrium: **1**-P_2 + 1,3-CHD ⇌ **1**-$P_2C_6H_8$; when naked [**1**-P_2] is generated, it either dimerizes, or it follows non-productive decomposition pathways. The decomposition products display broad features in their ^1H NMR spectra, and no detectable ^{31}P NMR or EPR signal. A better yield for the conversion of diphosphane **1**-$P_2C_6H_8$ to the tetraphosphane P_4**1**$_2$ was achieved when all volatile materials were removed directly from a freshly prepared solution of **1**-$P_2C_6H_8$. In this case, removal of the 1,3-cyclohexadiene evidently drives the equilibrium towards formation of P_4**1**$_2$, with a spectroscopic yield of 30% as measured by ^1H and ^{31}P NMR spectroscopy and referenced to PPh_3 as an internal standard.

The relative instability of **1**-$P_2C_6H_8$ has prevented its isolation as a solid. **1**-$P_2C_6H_8$ displays only one ^{31}P NMR signal, a singlet resonance, suggesting the selective formation of either the *exo* or the *endo* cycloaddition product. To obtain more information on the identity of the Diels–Alder isomer produced, we turned to theoretical methods. Structural models for the *exo*-**1**-$P_2C_6H_8$ and *endo*-**1**-$P_2C_6H_8$ isomers were built and optimized using DFT methods.[23] The calculated enthalpies of formation for the two isomers favor the formation of the *endo*-**1**-$P_2C_6H_8$ cycloaddition product by 12 kcal mol^{-1} (see Fig. 3). In this regard, the $[C_6H_8P_2]$ moiety is reminiscent of norbornadiene, which commonly chelates to metal ions using both C=C bonds.[32] The computational analysis revealed no bond critical point between Nb and

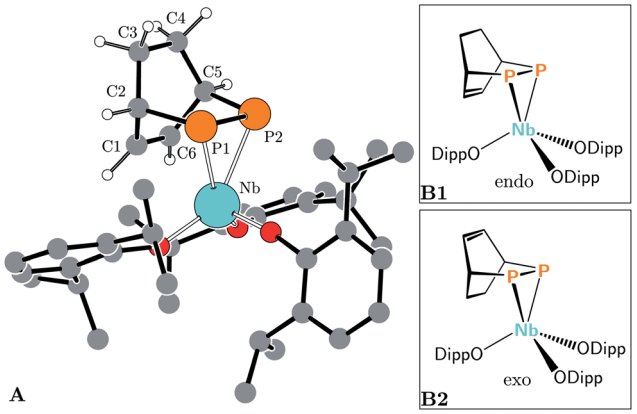

Fig. 3 (A) Model of the *endo*-**1**-$P_2C_6H_8$ Diels–Alder cycloaddition product optimized using DFT methods[23] and visualized using PLATON.[17] Selected interatomic distances (Å) and angles (°): P1–P2 2.213, Nb–P1 2.576, Nb–P2 2.575, Nb–C1 2.685, Nb–C6 2.703, P1–Nb–P2 50.92, Nb–P1–C5–C2 64.09. (B1) *Endo* isomer of **1**-$P_2C_6H_8$. (B2) *Exo* isomer of **1**-$P_2C_6H_8$.

the C atoms involved in the C=C double bond in the *endo*-**1**-$P_2C_6H_8$ isomer,[22] and the Nb–C distances of 2.685 and 2.703 Å are significantly larger than 2.22 Å, the sum of the covalent single-bond radii of the two elements.[18] Formally d^0, the niobium center in adduct **1**-$P_2C_6H_8$ cannot conventionally d–π* back-bond into a C=C double bond.[33] The Nb–olefin interaction in **1**-$P_2C_6H_8$ is therefore expected to be weak.

Pyridine-*N*-oxide has been employed previously to liberate unsaturated phosphorus ligands from niobium,[29] and here we took this approach in order to liberate the unsaturated cyclic diphosphene moiety $[(C_6H_8)P_2]$ from niobium. Accordingly, upon carrying out the generation of **1**-$P_2C_6H_8$ in the presence of pyridine-*N*-oxide (1 equiv.) the known *double* Diels–Alder adduct $P_2(C_6H_8)_2$[30] was observed to form in *ca.* 45% spectroscopic yield (Scheme 1, bottom). The previously reported oxo dimer O_2**1**$_2$[34] formed as a co-product.

Concluding remarks

In conclusion, we have developed a novel "2(3−1)" route to assemble the square, *cyclo*-P_4 ligand in P_4**1**$_2$. We have also accumulated circumstantial evidence pointing to the intermediacy of a mononuclear diphosphorus complex, obtained transiently by formal P^- abstraction from anion [**1**-P_3]$^-$.

Acknowledgements

This material is based upon work supported by the National Science Foundation under CHE-0719157 and CHE-1111357. For support including a gift of white phosphorus we thank Thermphos International. We thank Dr. Anthony F. Cozzolino and Daniel Tofan for assistance with computations and crystallography, respectively.

References

1 (*a*) W. Reppe, O. Schlichting, K. Klager and T. Toepel, *Justus Liebigs Ann. Chem.*, 1948, **560**, 1–92; (*b*) G. G. Melikyan and K. M. Nicholas, *Modern Acetylene Chemistry*, VCH, 1995, p. 99.

2 K. Dillon, F. Mathey and J. Nixon, *Phosphorus: the carbon copy: from organophosphorus to phospha-organic chemistry*, John Wiley, 1998.
3 (*a*) B. M. Cossairt, N. A. Piro and C. C. Cummins, *Chem. Rev.*, 2010, **110**, 4164–77; (*b*) M. Caporali, L. Gonsalvi, A. Rossin and M. Peruzzini, *Chem. Rev.*, 2010, **110**, 4178–4235.
4 (*a*) C. Esterhuysen and G. Frenking, *Chem.–Eur. J.*, 2003, **9**, 3518–3529; (*b*) N. A. Piro and C. C. Cummins, *J. Am. Chem. Soc.*, 2008, **130**, 9524–9535.
5 (*a*) G. Rathenau, *Physica*, 1937, **4**, 503–514; (*b*) M. E. Barr, B. R. Adams, R. R. Weller and L. F. Dahl, *J. Am. Chem. Soc.*, 1991, **113**, 3052–3060.
6 D. Tofan and C. C. Cummins, *Angew. Chem., Int. Ed.*, 2010, **49**, 7516–7518.
7 M. E. Barr and L. F. Dahl, *Organometallics*, 1991, **10**, 3991–3996.
8 O. J. Scherer, T. Volmecke and G. Wolmershauser, *Eur. J. Inorg. Chem.*, 1999, 945–949.
9 B. M. Cossairt, M.-C. Diawara and C. C. Cummins, *Science*, 2009, **323**, 602–602.
10 J. R. Strickler, P. A. Wexler and D. E. Wigley, *Organometallics*, 1988, **7**, 2067–2069.
11 J. S. Figueroa and C. C. Cummins, *J. Am. Chem. Soc.*, 2003, **125**, 4020–4021.
12 E. Niecke and R. Ruger, *Angew. Chem.*, 1983, **95**, 154–155.
13 C. E. Laplaza, W. M. Davis and C. C. Cummins, *Angew. Chem., Int. Ed. Engl.*, 1995, **34**, 2042–2044.
14 W. Seidel, O. Summerscales, B. Patrick and M. Fryzuk, *Angew. Chem., Int. Ed.*, 2009, **48**, 115–117.
15 F. H. Stephens, PhD Thesis, Massachusetts Institute of Technology, 2004.
16 A. S. P. Frey, F. G. N. Cloke, P. B. Hitchcock and J. C. Green, *New J. Chem.*, 2011, **35**, 2022–2026.
17 A. L. Spek, *J. Appl. Crystallogr.*, 2003, 7–13.
18 P. Pyykkö and M. Atsumi, *Chem.–Eur. J.*, 2009, **15**, 186–197.
19 F. Kraus, J. C. Aschenbrenner and N. Korber, *Angew. Chem., Int. Ed.*, 2003, **42**, 4030–4033.
20 (*a*) F. Sanz and J. J. Daly, *J. Chem. Soc. (A)*, 1971, 1083–1086; (*b*) J. C. J. Bart, *Acta Crystallogr., Sect. B: Struct. Crystallogr. Cryst. Chem.*, 1969, **B25**, 762–770; (*c*) W. Weigand, A. W. Cordes and P. N. Swepston, *Acta Crystallogr., Sect. B: Struct. Crystallogr. Cryst. Chem.*, 1981, **B37**, 1631–1634; (*d*) R. C. Smith, E. Urnezius, K.-C. Lam, A. L. Rheingold and J. D. Protasiewicz, *Inorg. Chem.*, 2002, **41**, 5296–9.
21 Xaim analysis revealed no bond critical points between these atoms. Additionally, the calculated Mayer bond orders were smaller than 0.3.
22 Analysis of critical points was carried out using the Xaim software developed by Jose Carlos Ortiz and Carles Bo, Universitat Rovira i Virgili, Tarragona, Spain.
23 F. Neese, *ORCA – an ab initio, Density Functional and Semiempirical program package, Version 2.8.0*, University of Bonn, 2009.
24 The calculated Mayer bond orders in the *cyclo*-P_4 ligand range from 0.69 to 0.74. The Mayer bond orders between Nb and P for six bonding interactions range from 0.62 to 0.88.
25 G. Schaftenaar and J. Noordik, *J. Comput.-Aided Mol. Des.*, 2000, **14**, 123–134.
26 A.-R. Allouche, *J. Comput. Chem.*, 2011, **32**, 174–182.
27 P. Pyykkö and M. Atsumi, *Chem.–Eur. J.*, 2009, **15**, 12770–12779.
28 J. D. Masuda, W. W. Schoeller, B. Donnadieu and G. Bertrand, *Angew. Chem., Int. Ed.*, 2007, **46**, 7052–7055.
29 B. M. Cossairt and C. C. Cummins, *Angew. Chem. Int. Ed.*, 2010, **49**, 1595–1598.
30 N. A. Piro, J. S. Figueroa, J. T. McKellar and C. C. Cummins, *Science*, 2006, **313**, 1276–1279.
31 L. Weber, *Chem. Rev.*, 1992, **92**, 1839–1906.
32 (*a*) K. Itoh, N. Oshima, G. B. Jameson, H. C. Lewis and J. A. Ibers, *J. Am. Chem. Soc.*, 1981, **103**, 3014–3023; (*b*) F. A. Cotton and J. H. Meadows, *Inorg. Chem.*, 1984, **23**, 4688–4693; (*c*) T. J. Chow, M.-Y. Wu and L.-K. Liu, *J. Organomet. Chem.*, 1985, **281**, c33–c37; (*d*) M. Dartiguenave, L. C. Ananias de Carvalho, Y. Dartiguenave, F. Belanger-Gariepy, M. Simard and A. L. Beauchamp, *J. Organomet. Chem.*, 1987, **326**, 139–149; (*e*) F. W. Grevels, J. Jacke, P. Betz, C. Krueger and Y. H. Tsay, *Organometallics*, 1989, **8**, 293–298.
33 J.-F. Carpentier, Z. Wu, C. W. Lee, S. Stromberg, J. N. Christopher and R. F. Jordan, *J. Am. Chem. Soc.*, 2000, **122**, 7750–7767.
34 V. M. Visciglio, P. E. Fanwick and I. P. Rothwell, *Acta Crystallogr., Sect. C: Cryst. Struct. Commun.*, 1994, **50**, 900–902.

